Nanoparticles with Dual Responses to Oxidative Stress and Reduced pH for Drug Release and Anti-inflammatory Applications

Hsiao-Lan Pu,[⊥,†] Wei-Lun Chiang,[⊥,†] Barnali Maiti,[†] Zi-Xian Liao,[†] Yi-Cheng Ho,[‡] Min Suk Shim,[§] Er-Yuan Chuang,[†] Younan Xia,[§] and Hsing-Wen Sung[†,*]

[†]Department of Chemical Engineering and Institute of Biomedical Engineering, National Tsing Hua University, Hsinchu 30013, Taiwan (ROC), [‡]Department of Biotechnology, Vanung University, Taoyuan 32061, Taiwan (ROC), and [§]The Wallace H. Coulter Department of Biomedical Engineering, Georgia Institute of Technology and Emory University, Atlanta, Georgia 30332, United States. [⊥]H.-L. Pu and W.-L. Chiang contributed equally to this work.

ABSTRACT

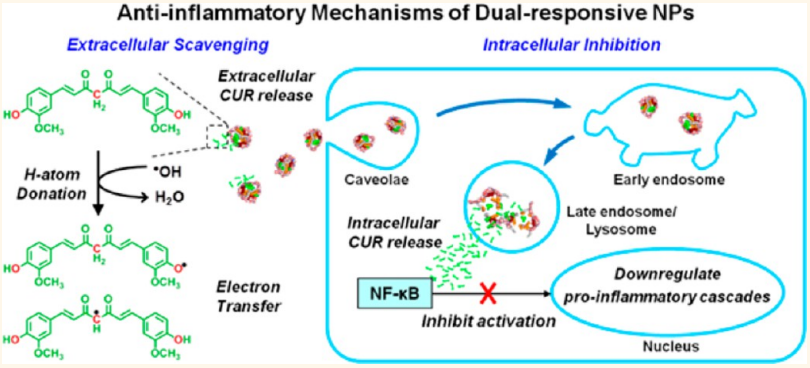

Oxidative stress and reduced pH are involved in many inflammatory diseases. This study describes a nanoparticle-based system that is responsive to both oxidative stress and reduced pH in an inflammatory environment to effectively release its encapsulated curcumin, an immune-modulatory agent with potent anti-inflammatory and antioxidant capabilities. Because of the presence of Förster resonance energy transfer between curcumin and the carrier, this system also allowed us to monitor the intracellular release behavior. The curcumin released upon triggering could efficiently reduce the excess oxidants produced by the lipopolysaccharide (LPS)-stimulated macrophages. The feasibility of using the curcumin-loaded nanoparticles for anti-inflammatory applications was further validated in a mouse model with ankle inflammation induced by LPS. The results of these studies demonstrate that the proposed nanoparticle system is promising for treating oxidative stress-related diseases.

KEYWORDS: antioxidant · anti-inflammation · reactive oxygen species · reactive nitrogen species · drug delivery

As the first response of the immune system to infection and/or irritation, inflammation is associated with many diseases including cancer, atherosclerosis, asthma, and cystic fibrosis.[1,2] Its signature features include the presence of oxidative stress (*i.e.*, overproduction of oxidants such as ·OH and $ONOO^-$ from H_2O_2 and ·NO, respectively) and reduction of pH.[3,4] The oxidants derived from reactive oxygen species (ROS) like H_2O_2 and reactive nitrogen species (RNS) such as ·NO are highly reactive toward DNA, proteins, and lipids, causing significant destruction to the cells.[5,6] In inflamed tissues, the activated macrophages also produce a variety of ROS/RNS intracellularly. When produced in excess, these oxidants will spill out and exert extracellular toxicity to the surrounding tissues through lipid peroxidation and DNA damage.[7]

From the therapeutic perspective, one of the major challenges lies in the development of carriers that can effectively release bioactive agents selectively to the areas under oxidative stress, and in particular, are capable of cytoplasmic delivery. Here we

* Address correspondence to hwsung@che.nthu.edu.tw.

Received for review July 29, 2013 and accepted January 3, 2014.

Published online January 03, 2014
10.1021/nn4058787

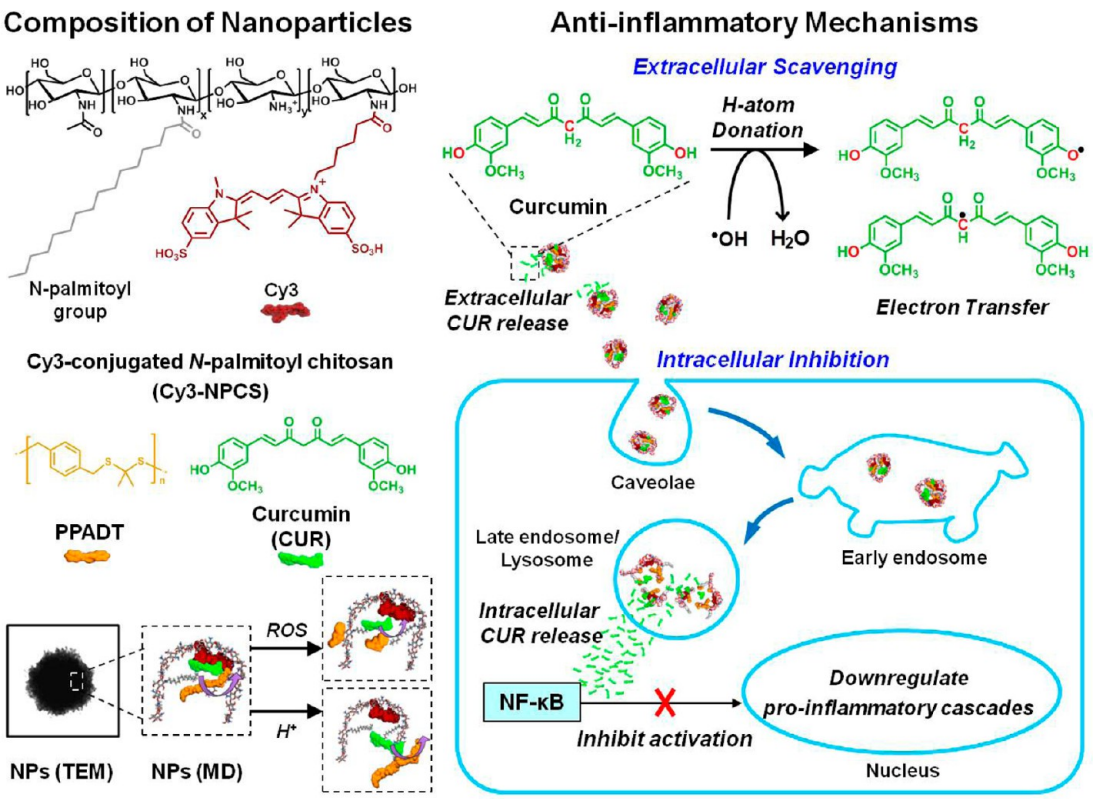

Figure 1. Schematic illustrations showing the composition/structure of the dual-responsive nanoparticles developed in this study and their extracellular/intracellular anti-inflammatory mechanisms.

report a new system based on smart nanoparticles (NPs) that can be triggered by oxidative stress and reduced pH to effectively deliver the encapsulated payload, curcumin, to inflamed tissues to inhibit the overproduction of ROS/RNS. As a hydrophobic, fluorescent molecule isolated from the rhizome of turmeric, curcumin has potent anti-inflammatory and antioxidant activities. Specifically, curcumin plays a critical role in controlling the signal transduction pathways involved in inflammatory responses through the down-regulation of inflammatory transcription factors such as nuclear factor kappa B (NF-κB).[8] Curcumin is also a powerful scavenger of free-radical oxidants *via* H-atom donation and electron transfer,[9] exerting its antioxidant activity.

Stimuli-responsive NPs have received considerable attention as a smart drug-delivery system for various therapeutic applications.[10−12] In this study, pH-responsive NPs made of *N*-palmitoyl chitosan (NPCS) that bears a hydrophobic Cy3 moiety were explored as a carrier for the delivery of curcumin. To make the carrier simultaneously responsive to pH and oxidative stress, we also encapsulated poly-(1,4-phenyleneactone dimethylene thioketal) (PPADT), a hydrophobic copolymer derived from 1,4-benzenedimethanethiol and 2,2-dimethoxypropane monomers, in the NPs. Since PPADT contains thioketal linkages, it can be selectively degraded into hydrophilic fragments in response to ROS while remaining to be stable in an environment containing an acid, base, or protease.[13]

Figure 1 shows a schematic illustration of the dual-responsive NPs and their mechanisms in disabling the excess ROS/RNS produced by the lipopolysaccharide (LPS)-stimulated macrophages responsible for inflammation. In the presence of curcumin and PPADT, NPCS can self-assemble into NPs in a neutral aqueous solution primarily due to the hydrophobic interaction between its conjugated *N*-palmitoyl group and Cy3 moiety. This associated polyelectrolyte (Cy3-NPCS) can undergo a conformational change upon triggering by the environmental pH, as determined by a balance between charge−charge repulsions of the protonated amine groups on NPCS and hydrophobic interactions of the side chains.[14] Additionally, in response to oxidative stress, the encapsulated hydrophobic PPADT can degrade into hydrophilic fragments, making the NPs unstable and thus disintegrated. Furthermore, the encapsulated curcumin and conjugated Cy3 could serve as the donor and acceptor, respectively, for Förster resonance energy transfer (FRET) to help localize the NPs and monitor the intracellular release of curcumin. The FRET involves the nonradiative transfer of energy from the excited state of a donor (curcumin) to the empty levels of an acceptor (Cy3) placed in close proximity (<10 nm), and its efficiency can thus be used to resolve the separation between the donor and acceptor.[15]

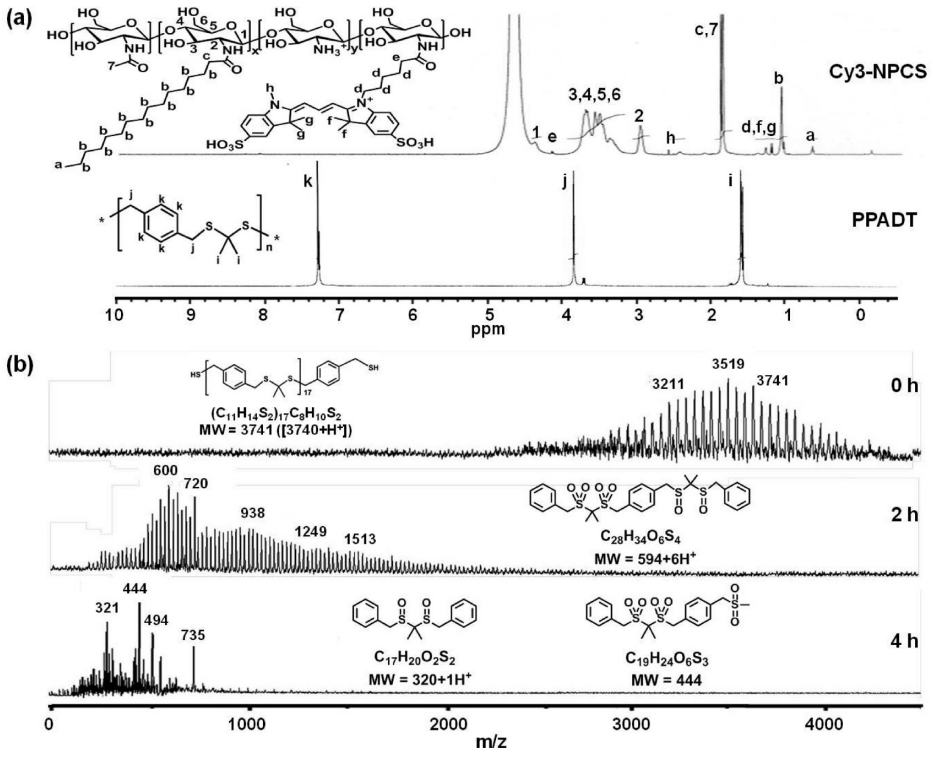

Figure 2. (a) ^{1}H NMR spectra of the synthesized Cy3-NPCS and PPADT. (b) Degradation of PPADT in the ROS environment with time, evaluated by MALDI-TOF mass spectrometry. The formula in Figure 2b (at t = 2 h and 4 h) show some of the possible compounds that could be generated when PPADT went through degradation in the ROS environment.

RESULTS AND DISCUSSION

Characteristics of Cy3-NPCS, PPADT, and Test NPs. The synthesized Cy3-NPCS and PPADT were characterized by ^{1}H NMR (Figure 2a). The appearance of alkyl protons in the spectrum of Cy3-NPCS indicates that the palmitoyl group (a, b, c) and Cy3 moiety (d, e, f, g) were successfully conjugated to the free amine groups of chitosan (1, 2, 3, 4, 5, 6); their degrees of substitutions on the amine groups were approximately 15.0 and 3.4%, respectively. Geminal dimethyl protons (i) along with benzylic protons (j, k), as observed in the PPADT spectrum, suggest that 1,4-benzenedimethanethiol and 2,2-dimethoxypropane monomers had been effectively polymerized, and the average molecular weight was around 3700 Da as estimated from the MALDI-TOF mass spectra.

To examine its sensitivity to ROS, we treated the as-prepared PPADT with 1 mM of H_2O_2 and analyzed the molecular weights of the resultant products using MALDI-TOF mass. As shown in Figure 2b, PPADT degraded from 3700 Da to approximately 500 Da over a period of 4 h, indicating its sensitivity to oxidative stress. The prepared NPs were 258.6 ± 105.0 nm in diameter with a zeta potential of 7.2 ± 4.1 mV at pH 7.4 (n = 6). The loading efficiencies (loading contents) of curcumin and PPADT were about 55% (5%) and 75% (12%), respectively, as determined using high performance liquid chromatography (HPLC) and inductively coupled plasma mass spectrometry (ICPMS). Accordingly, the number of dyes (Cy3)/drugs (curcumin) per particle was estimated to be approximately 1/130 by molar ratio.

Sensitivity of Test NPs to Oxidative Stress and Reduced pH. Since high proton (down to pH 5.4) and ROS (up to 1 mM H_2O_2) concentrations have been reported in inflamed tissues,[3,4] the sensitivity of the formulated NPs to oxidative stress was characterized in a buffer solution (pH 5.5) containing 1 mM H_2O_2. The effects of these two environmental stimuli were also investigated separately. The morphological changes of NPs in response to the inflammatory stimuli were examined by transmission electron microscopy (TEM). Under the physiological environment (pH 7.4), most amine groups on the main chain of NPCS were deprotonated, and the hydrophobic interaction between the palmitoyl and Cy3 side chains dominated, causing the NPs to condense (Figure 3a). When incubated in an environment of oxidative stress (1 mM H_2O_2) or at a reduced pH (pH 5.5), the test NPs were swollen. After incubation for 4 h, their sizes increased to 327.9 ± 150.6 and 344.1 ± 145.5 nm, respectively (P < 0.05), indicative of their responsiveness to each of the environmental stimuli investigated. Conversely, the NPs were gradually disintegrated under a synergic effect between oxidative stress and reduced pH that mimics the inflammatory milieu. The transition from a condensed to a disintegrated structure enabled the formulated NPs to function as a smart capsule to release the drug locally in response to the environmental stimuli.

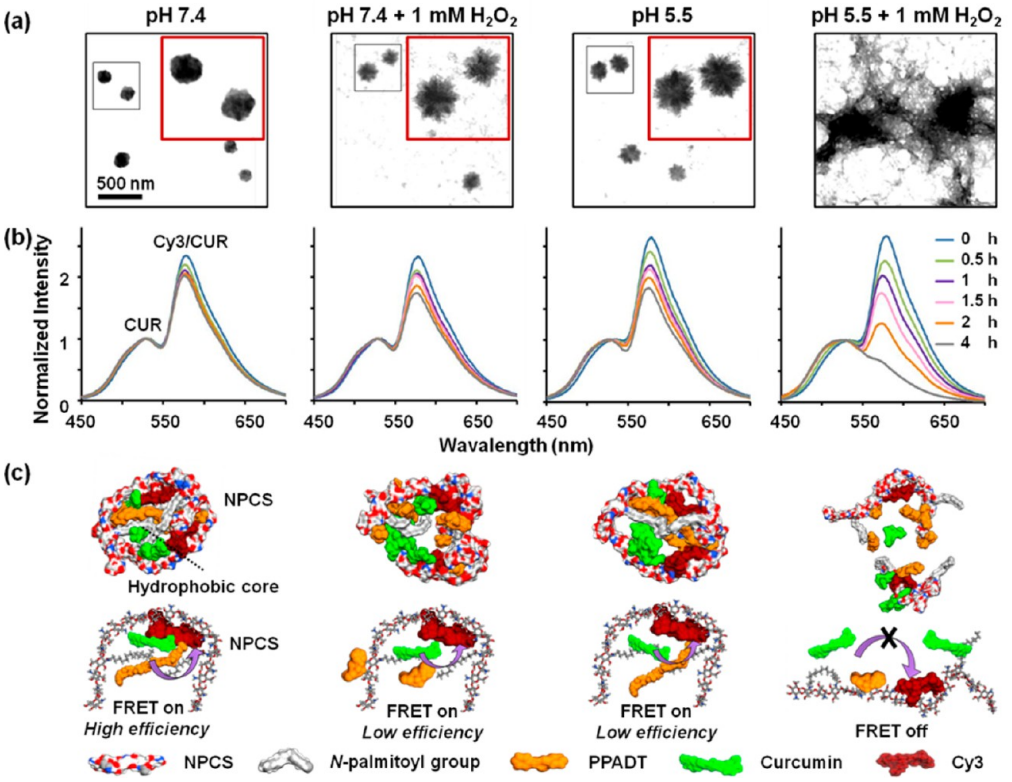

Figure 3. (a) TEM micrographs of the formulated NPs present in each studied environment after they had been dried. Area defined by a square is shown at a higher magnification in the inset. (b) In response to the oxidative stress and reduced pH, the NPs showed sequential decrease in FRET efficiency with time. (c) Results of MD simulations showing the changes in internal structure of the NPs and their subsequent FRET efficiencies. CUR: curcumin.

TABLE 1. Changes in FRET Efficiency for the NPs Containing Curcumin That Had Been Exposed to Different Environmental Stimuli[a]

environmental stimuli		pH 7.4	pH 7.4 + 1 mM H_2O_2	pH 5.5	pH 5.5 + 1 mM H_2O_2
peak ratio Cy3/CUR	at 0 h	2.3 ± 0.1	2.3 ± 0.2	2.6 ± 0.2	2.7 ± 0.2
	at 4 h	2.0 ± 0.2	1.7 ± 0.3	1.8 ± 0.3	0.6 ± 0.2
FRET efficiency		86.3 ± 5.2%	74.2 ± 6.7%	69.3 ± 7.2%	23.2 ± 5.3%

[a] The FRET efficiency of the test NPs was calculated on the basis of their emission ratio of Cy3/curcumin (CUR) observed at 4 h following exposure relative to that before exposure (0 h) ($n = 5$).

Figure 3b shows the FRET spectra taken from aqueous suspensions of the NPs containing curcumin after they had been incubated for distinct periods of time under different combinations of environmental stimuli. The peaks were normalized to the maximum intensity of curcumin (the donor) at *ca.* 529 nm. All spectra were obtained by irradiating the NP suspensions with a monochromic light at 420 nm, corresponding to the excitation wavelength of curcumin, the FRET donor. The Cy3 and Cy3-NPCS (NPs with no curcumin) were used as controls. According to the results shown in Supplementary Figure S1, no significant changes in Cy3 quantum yield of Cy3 and Cy3-NPCS were observed in response to distinct environmental stimuli throughout the study. Conversely, for test NPs containing curcumin, we observed a sequential decrease in the emission ratio of Cy3 to curcumin with time in the presence of oxidative stress and reduced pH due to the drop in FRET efficiency (Table 1), suggesting a gradual disintegration of test NPs.

We also used molecular dynamic (MD) simulations to understand the change in internal structure for the NPs and their subsequent FRET efficiency, as triggered by the inflammatory stimuli. At the physiological environment (pH 7.4), a hydrophobic core, which was composed of the palmitoyl and Cy3 chains and the loaded PPADT and curcumin, was present inside the formulated NPs (Figure 3c). In this case, the curcumin molecules were in close proximity to the conjugated Cy3 moieties, resulting in an efficient energy transfer between them (*i.e.*, FRET on). At the inflammation environment, the NPs became disintegrated gradually and the curcumin molecules were no longer accessible to the conjugated Cy3 moieties for energy transfer (*i.e.*, FRET off).

Intracellular Release Behavior of Curcumin. Our previous study found that the NPs made of NPCS could be

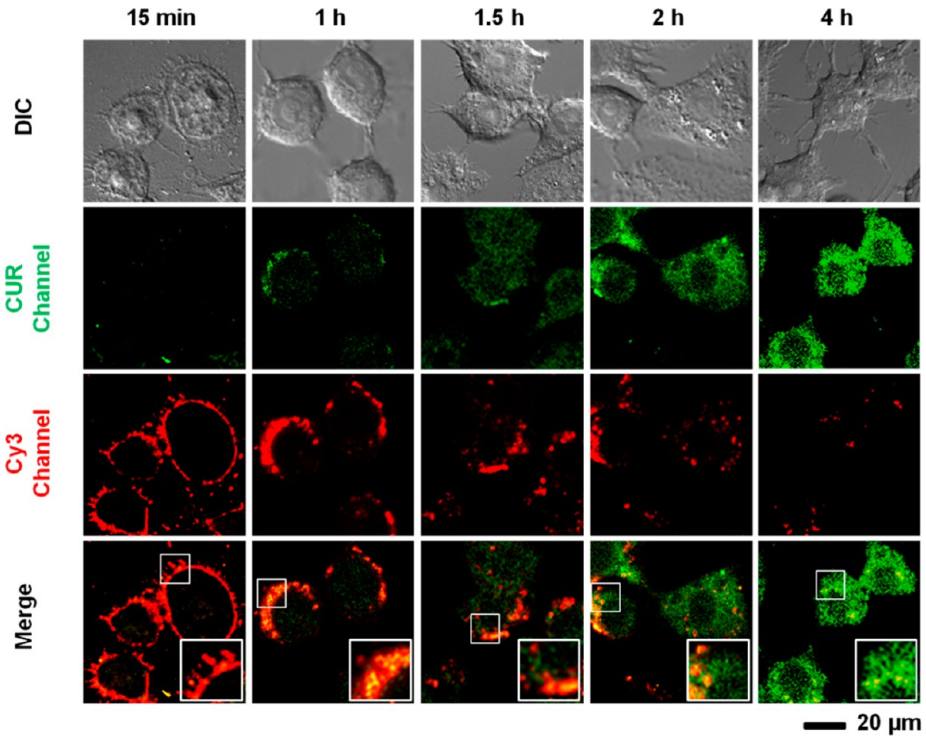

Figure 4. CLSM images showing the cellular uptake of the formulated NPs and their intracellular drug release behaviors, as monitored using the FRET technique. The inset in each panel shows a higher magnification image. CUR: curcumin.

internalized into cells within 15 min after incubation *via* a caveolae-mediated pathway.[14] Following endocytosis, the NPCS NPs were trafficked intracellularly from neutral (caveolae with pH 7.0 at 15 min) to acidic organelles (early endosomes with pH 6.2 at 1−1.5 h and late endosomes/lysosomes with pH 5.0 at 2−4 h).[14] We investigated the feasibility of using FRET to monitor the uptake of the formulated NPs and their drug release behaviors intracellularly by imaging with confocal laser scanning microscopy (CLSM). In this study, LPS-stimulated macrophage RAW264.7 cells were incubated with the NPs for different durations of time. Fluorescence images were taken in optical windows between 500−550 nm (curcumin imaging channel, green color) and 570−620 nm (Cy3 imaging channel, red color) when the samples were irradiated at 488 nm.[16,17]

At 15 min postincubation, red fluorescence indicative of intact NPs was observed in the Cy3 imaging channel (FRET on with high efficiency, Figure 4). With time progressing (1−2 h), a significant decrease in red fluorescence for Cy3 was seen (FRET on with low efficiency), while some green fluorescence was observed within the cytosol, indicating the release of curcumin from the test NPs. By 4 h, the Cy3 fluorescence was almost diminished (FRET off) and the green fluorescence of curcumin became much stronger, suggesting disintegration of the NPs and a significant release of curcumin intracellularly. It is important to deliver the poorly bioavailable curcumin into the cells to exert its anti-inflammatory activity since its main mechanism of action is to inhibit the activation of NF-κB and downregulate the proinflammatory cascades.[18]

***In Vitro* Drug Release Profiles.** Figure 5a displays the release profiles of curcumin from the formulated NPs under distinct environments. At the physiological pH 7.4, the extent of curcumin released from the NPs was relatively low, implying their stability during blood circulation. Once at the inflammatory milieu, approximately 10% of the initial content of the encapsulated curcumin was released within the first 15 min; the drug was constantly released with time, and 50% of the encapsulated curcumin was liberated at 4 h after incubation, because of the disintegration of NPs. These results suggest that the release of curcumin from the formulated NPs was dependent on oxidative stress and reduced pH and could occur intracellularly and extracellularly. This feature is of particular interest in overcoming the excess oxidants in inflamed tissues.

Inhibitory Effects on Excess Oxidants. As essential physiological regulators, ROS/RNS normally exist in cells in balance with antioxidant molecules.[19] A well-defined model of macrophage activation at sites of inflammation is the treatment of RAW264.7 cells with LPS, resulting in the overproduction of oxidants and thus irreversible oxidative cellular damage.[20−22] In the present study, RAW264.7 cells were pretreated with 1 μg mL^{-1} of LPS[23,24] for 24 h to generate ROS/RNS and then treated with either free-form curcumin or the curcumin-loaded NPs; the group without any treatment was used as a control. Their inhibitory effects on ROS (H_2O_2) and RNS ($\cdot$NO) overproductions were

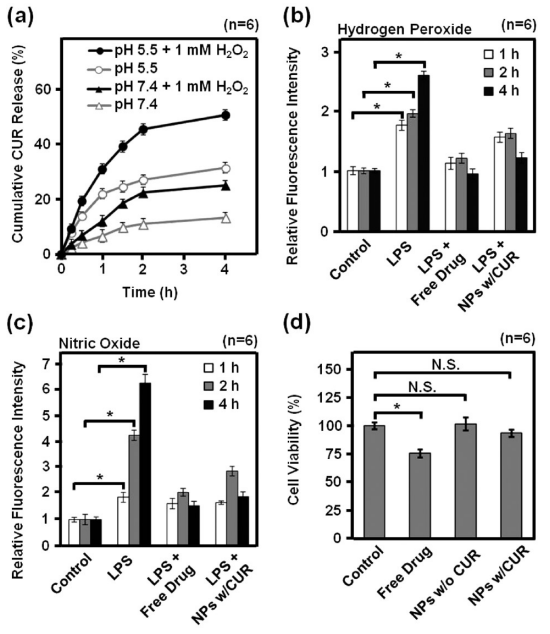

Figure 5. (a) *In vitro* release profiles of curcumin (CUR) from the test NPs in distinct environments (n = 6). (b,c) The anti-inflammatory activities of the formulated NPs when exposed to environments with excess ROS and RNS, respectively, in the oxidative-stress areas (n = 6). (d) Quantitative results of cell viability evaluated by the MTT assay (n = 6). N.S.: not significant; *: statistically significant (P < 0.05).

examined at predetermined time intervals based on the Amplex Red assay and the Griess reaction, respectively.[25,26] The overproductions of H_2O_2 and ·NO and accumulations of their derived oxidants are implicated in numerous diseases.[5,6]

As shown in Figure 5b and c, the cells activated by LPS led to excess production of ROS/RNS when compared to the control group without any treatment; at 24 h poststimulation, productions of 2.6-fold H_2O_2 and 6.3-fold ·NO were observed (P < 0.05). The inhibitory effects of free-form curcumin on reducing the levels of excess ROS/RNS showed a concentration-dependent manner (data not shown), with complete inhibition of LPS-induced ROS/RNS overproduction to the normal levels being achieved at 25 μM of free-from curcumin in 4 h. Therefore, the concentration of 25 μM curcumin was used in the study. Previous studies have demonstrated that curcumin is a potent immune-modulatory agent that can modulate the activation of macrophages.[8] The curcumin-loaded NPs (25 μM curcumin) could also effectively reduce the overproductions of ROS/RNS (down to 1.1-fold H_2O_2 and 1.5-fold ·NO, respectively), as a result of the synergy effects of free-radical scavenging extracellularly and inhibition of the oxidant overproduction intracellularly.[27,28]

To examine the cytotoxicity, we incubated RAW264.7 macrophages with the test NPs (with or without loading of curcumin) for 24 h; the viability of cells treated with free-form curcumin and that without any treatment were used as controls. The concentration of free-form curcumin used was equivalent to what was loaded in the NPs (25 μM curcumin).[29,30] The mitochondrial activity of living cells was then measured by the MTT assay.[31] According to the results shown in Figure 5d, a low cytotoxicity was observed for the group treated with free-form curcumin (P < 0.05); it has been reported that curcumin at low concentrations can actually increase the level of ROS.[32] Conversely, no significant cytotoxicity was observed for groups receiving the NPs with or without loading of curcumin (P > 0.05).

***In Vivo* Biodistribution of Curcumin.** To gain an insight into its *in vivo* biodistribution, free-form curcumin and the curcumin-loaded NPs were separately injected into the ankles of mice in which acute inflammation had been chemically induced by LPS; the ankles of healthy mice were used as controls. Following the injections, the arising fluorescence of curcumin in the test ankles was imaged by using an *in vivo* imaging system (IVIS), and their relative intensity (the intensity that was normalized to that before injection) was calculated.

According to the results shown in Figure 6a and b, a gradual decrease in the fluorescence intensity in both healthy and inflamed ankles was observed in the group that received the free-form curcumin (P < 0.05), suggesting that the free-form drug could not be effectively retained at the site of injection. There was no significant change in fluorescence intensity in the healthy ankles treated with the curcumin-loaded NPs (P > 0.05). Conversely, the intensity of fluorescence in the inflamed ankles that received the test NPs was substantially elevated, indicating that the injected NPs could be effectively triggered to release their encapsulated curcumin *via* the oxidative stress and reduced pH present in inflamed tissues.

***In Vivo* Anti-inflammatory Activity.** To further evaluate the feasibility of using these curcumin-loaded NPs for anti-inflammatory applications through direct local injection, the mouse model with ankle inflammation induced by LPS was employed. A luminescent probe, L-012, was applied *via* intravenous administration for *in vivo* detection of ROS/RNS related to inflammation.[33,34] Because of its high sensitivity toward ROS/RNS, L-012 has been used extensively as a ROS/RNS-sensing probe to detect *in vivo* inflammation.[34] Figure 6c and Supplementary Figure S2 show representative images obtained using an IVIS for luminescence emitted from the healthy and inflamed ankles treated with saline, free-form curcumin, or test NPs containing curcumin; the luminescence signals were expressed in p s^{-1} cm^{-2} sr^{-1}. As shown, negligible chemiluminescence emission was identified at the healthy ankle, which was not given LPS. However, the inflamed ankles treated with free-form curcumin (a 66.7 ± 8.0% reduction) or test NPs containing curcumin (a 52.9 ± 12.7% reduction, n = 4, P < 0.05) revealed a significantly lower chemiluminescence emission when compared to the group that received saline, indicative of the decline of the local concentrations of

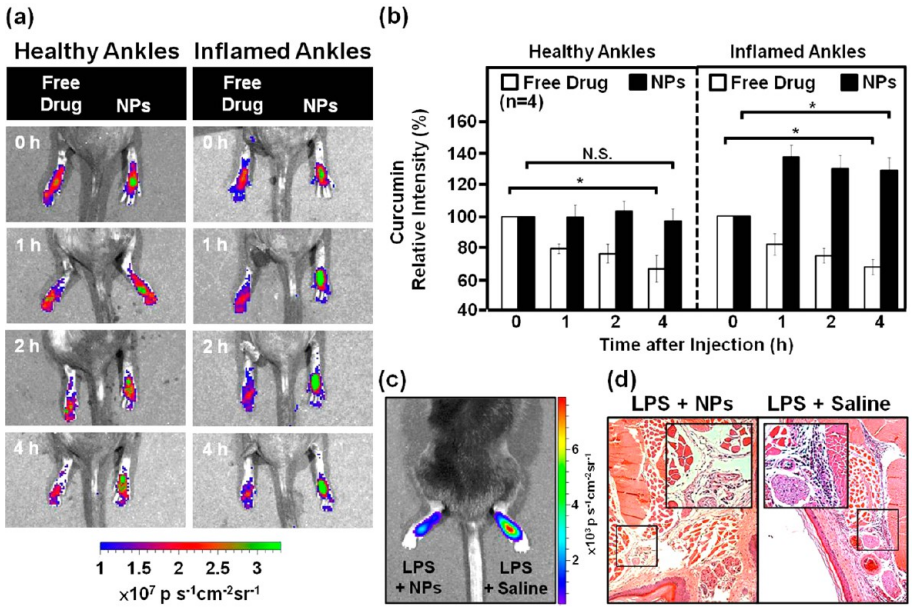

Figure 6. *In vivo* **biodistribution of curcumin: (a) fluorescence signals of healthy and inflamed ankles treated with free-form curcumin and the curcumin-loaded NPs, and (b) their relative fluorescence intensities *versus* time. The anti-inflammatory effects of the formulated NPs on the ankle inflammation induced by LPS in a mouse model: (c) IVIS image, (d) photomicrographs stained by H&E. Insets show magnified views. N.S.: not significant; *: statistically significant ($P < 0.05$).**

ROS/RNS. Histological examination using ankle sections stained with hematoxylin–eosin (H&E) verified the rescue from LPS-induced inflammation for the group treated with the curcumin-loaded NPs (Figure 6d).

CONCLUSIONS

In summary, we have demonstrated that the formulated NPs can be triggered effectively by both oxidative stress and reduced pH in an inflammatory milieu to release their encapsulated curcumin. The NPs can also be used as an imaging probe to monitor the *in vitro* drug release behavior intracellularly by using a technique based on FRET. This dual-responsive nanoparticulate system is highly potent for the delivery of therapeutics to sites of inflammation to reduce the oxidative stress.

EXPERIMENTAL SECTION

Materials. Chitosan (50 kDa) with 85% deacetylation was purchased from Koyo Chemical (Tokyo, Japan). Curcumin, H_2O_2, LPS, 1,4-benzenedimethanethiol, 2,2-dimethoxypropane, benzene, *p*-toluenesulphonic acid, 2,2-dimethoxypropane, palmitic acid *N*-hydroxysuccinimide ester, hexane, dimethyl sulfoxide (DMSO), and MTT (3-(4,5-dimethylthiazol-2-yl)-2,5-diphenyl tetrazolium bromide) were obtained from Sigma-Aldrich (St. Louis, MO, USA). The Cy3-NHS was acquired from Invitrogen (Carlsbad, CA, USA). The luminescent probe L-012 was obtained from Wako Chemical (Neuss, Germany).

Synthesis and Characterization of PPADT[13]. A three-necked round bottle flask was charged with 1,4-benzenedimethanethiol (0.7 g, 4.1 mmol, 1.0 equiv) and 2,2-dimethoxypropane (0.43 g, 4.1 mmol, 1.0 equiv) in dry benzene and then equipped with a metering funnel and distillation head for removal of the methanol byproduct. The mixture was subsequently heated to 100 °C. In the heated mixture, a catalytic *p*-toluenesulphonic acid (0.004 g, 0.005 equiv) in distilled ethyl acetate was added to initiate the reaction. The funnel stopcock was set so that a small amount of 2,2-dimethoxypropane (0.08 equiv h^{-1}) was added dropwise over a period of 12 h. After the reaction, the resulting polymer was precipitated in cold hexane.

The polymer was dried in a vacuum and analyzed by ^{1}H NMR, ^{13}C NMR (Varian Unityionva 500 NMR Spectrometer, MO, USA), MALDI-TOF (Micromass, UK), Fourier transformed infrared (FT-IR; Perkin-Elmer Spectrum RX 1 FT-IR System, Buckinghamshire, UK) spectroscopy, and gel permeation chromatography (GPC; RI2000-F, SFD, Torrance, CA). For further structure confirmation, ^{1}H NMR and ^{13}C NMR of PPADT were recorded with the following results: ^{1}H NMR (500 MHz, $CDCl_3$) δ ppm 7.28 (s, 4H), 3.85 (s, 4H), 1.60 (s, 6H); ^{13}C NMR (125 MHz, $CDCl_3$) δ ppm 129.54, 77.56, 77.25, 76.93, 35.03, 31.01; MALDI-TOF (ESI) MS *m/z* 3741 (MH^+); IR (cm^{-1}, KBr) 2958, 2919, 1510, 1429, 1363, 1110, 729, 630. The molecular weight of the resulting polymer was approximately 3700 Da with a polydispersity of 1.6, as determined by GPC.

Synthesis and Characterization of Cy3-NPCS[14]. CS (1 g, 6.0 mmol, 1 equiv) was dissolved in aqueous acetic acid (50 mL, 1% w/v). Subsequently, 1 N NaOH was slowly added in to adjust the pH value to 6.2; the final volume of CS solution was adjusted to 100 mL with the addition of deionized water. The mixture was heated to 98 °C. A solution of palmitic acid *N*-hydroxysuccinimide ester (0.4 g, 1.1 mmol, 0.2 equiv) in absolute ethanol was added dropwise to the heated mixture and stirred thoroughly for 36 h. After the reaction, the mixture was cooled to room temperature and then precipitated at pH 9.0. The obtained product was washed by acetone and then air-dried. Next, a solution of Cy3-NHS in DMSO (1 mg mL^{-1}) was prepared and added gradually into an aqueous NPCS (2 mg mL^{-1}) while stirring; the weight ratio of fluorescent dye to NPCS was kept at 1:50 (w/w). The reaction was maintained at pH 6.2 and stirred continuously for 12 h in the dark. The unconjugated fluorescent dye (free-form Cy3) was removed *via* dialysis against deionized water in the dark and replaced on a daily basis until no fluorescence was detected in the supernatant.

The synthesized Cy3-NPCS was analyzed by ^{1}H NMR and FT-IR spectroscopy; the degree of substitution on Cy3-NPCS was

determined by the ninhydrin assay. For further structure confirmation, ^{1}H NMR of Cy3-NPCS was recorded with the following results: ^{1}H NMR (Varian, 500 MHz, $CDCl_3$) δ ppm 4.44 (s, 15H), 4.19 (t, J = 7.0 Hz, 1H), 3.80−3.73 (m, 67H), 3.64−3.60 (m, 31H), 3.58−3.54 (m, 45H), 3.45−3.40 (m, 27H), 3.02 (s, 23H), 1.92 (s, 16H), 1.91 (s, 43H), 1.34 (s, 2H), 1.26 (s, 1H), 1.25 (s, 1H), 1.13 (s, 16H), 1.09 (s, 1H), 0.71 (t, J = 7.0 Hz, 1H); IR (cm^{-1}, KBr) 3432, 1736, 1560, 1442, 1200, 1115, 1027.

Preparation and Characterization of Test NPs. The as-synthesized Cy3-NPCS and PPADT were used to prepare the test NPs. The free curcumin and PPADT were removed by centrifugation. The NP suspensions were then analyzed by dynamic light scattering, TEM, and MD simulations[35] under distinct environments, and their FRET efficiency was determined using a fluorescence spectrometer (Spex FluoroMax-3, Horiba Jobin Yvon, Edison, NJ, USA).

The loading efficiencies and loading contents of curcumin and PPADT in the test NPs were determined by assaying their respective amounts left in the supernatants by using HPLC (Jasco, Tokyo, Japan) and ICPMS (SCIEX ELAN 5000, Perkin-Elmer, Waltham, USA). The drug loading efficiency and loading content were calculated using the equations shown below.[36]

$$\text{loading efficiency (\%)} = \frac{\text{total amount of drug added} - \text{free drug}}{\text{total amount of drug added}} \times 100\%$$

$$\text{loading content (\%)} = \frac{\text{total amount of drug added} - \text{free drug}}{\text{weight of NPs}} \times 100\%$$

MD Simulations. To illustrate the local conformational changes within the test NPs in response to each environmental stimulus, two sets of their constituent molecules were used in the MD simulations. The MD simulations were carried out using the program NAMD with parameters adapted from the CHARMM 27 force field.[37] The models were minimized to remove unfavorable contacts, brought to 310 K by velocity rescaling, and equilibrated for 1 ns. Before any MD trajectory was run, 40 ps of energy minimization were conducted to relax the structural tensions; this minimum structure was the starting point in the MD simulations.

Test molecules were placed into a cubic simulation box of 80 Å. A cutoff distance of 12 Å was used to calculate the nonbonded and electrostatic interactions. The heating process was carried out from 0 to 310 K through Langevin damping with a coefficient of 10 ps^{-1}. A time step of 2 fs was employed to rescale the temperature. After heating of 20 ps to 310 K, the equilibration trajectories of 1 ns were recorded, providing the data for the structural and thermodynamic evaluations. The equations of motion were integrated with the Shake algorithm with a time step of 1 fs. Figures of the atoms in molecules and their hydrogen bonds were produced using UCSF Chimera.[38]

Intracellular Monitoring of Curcumin Release. Following LPS stimulation for 24 h, RAW264.7 cells were incubated in a fresh medium containing the test NPs. At different time intervals, cells were washed twice with phosphate buffered saline, fixed in 4% paraformaldehyde, and examined by CLSM (TCS SL, Leica, Germany).

***In Vitro* Drug Release Study.** The NP suspensions present at distinct experimental conditions were centrifuged at predetermined time points. The amount of curcumin released from the test NPs was analyzed by HPLC.

Cytotoxicity Assay. Cells were cocultured with the test NPs for 24 h. Samples were then aspirated, and cells were incubated in a medium containing 1 mg mL^{-1} of MTT reagent for 4 h, followed by an addition of 1 mL of DMSO. Optical density readings were obtained using a multiwell scanning spectrophotometer (Dynatech Laboratories, Chantilly, VA, USA).

Anti-inflammatory Activity. Cells were stimulated by LPS for 24 h and then treated with a fresh DMEM medium containing either free-form curcumin or the test NPs. At predetermined time intervals, the medium was taken out for centrifugation, and the supernatant was assessed by the Amplex Red assay and the Griess reaction for quantification of H_2O_2 and ·NO, respectively.[39]

***In Vivo* Biodistribution of Curcumin.** Animal experiments were conducted in accordance with the national guidelines and approved by the Animal Care Committee of National Tsing Hua University, Taiwan. Inflammation was induced in each ankle of C57Bl/6 mice (4 weeks old) *via* the injection of 20 μL of LPS (2 mg mL^{-1}). At 4 h following LPS treatment, free-form curcumin and the NPs containing curcumin (0.25 mg kg^{-1}) were individually injected into the inflamed ankles; the healthy mice were used as controls. The fluorescence images of the ankles were then acquired using an IVIS imaging system (Xenogen, Alameda, CA, USA) with fluorescence excitation/emission wavelengths of 430/520 nm at 10 s acquisition. During *in vivo* imaging, the mice were immobilized using the anesthetic isoflurane (1.5−2.5%). The fluorescence intensity of each sample was calculated from the fluorescence signal (p s^{-1} cm^{-2} sr^{-1}) using the Living Image software Version (Xenogen, Alameda, CA, USA).

***In Vivo* Anti-inflammatory Activity.** At 4 h following LPS treatment, the NPs containing curcumin (0.25 mg kg^{-1}) was injected into one of the inflamed ankles; the other ankle receiving saline was used as a control. Four hours later, L-012 probe (75 mg kg^{-1}) was administered *via* tail vein injection; luminescence images of the inflamed ankles were then acquired using the IVIS imaging system. The luminescent camera was set to 1 min acquisition, blocked excitation filter, and open emission filter. Afterward, the animals were sacrificed, and the ankle joints were harvested and processed for histological analyses.

Statistical Analysis. Two groups were compared by the one-tailed Student's *t*-test using statistical software (SPSS, Chicago, IL, USA). Data are presented as mean ± SD. A difference of $P < 0.05$ was considered statistically significant.

Conflict of Interest: The authors declare no competing financial interest.

Acknowledgment. This work was supported by a grant from the National Science Council (NSC 100-2221-E-007-009), Taiwan (ROC).

Supporting Information Available: Supporting Figures S1 and S2. This material is available free of charge via the Internet at http://pubs.acs.org.

REFERENCES AND NOTES

1. Barnes, P. J. Immunology of Asthma and Chronic Obstructive Pulmonary Disease. *Nat. Rev. Immunol.* **2008**, *8*, 183–192.
2. Umetsu, D. T.; McIntire, J. J.; Akbari, O.; Macaubas, C.; DeKruyff, R. H. Asthma: An Epidemic of Dysregulated Immunity. *Nat. Immunol.* **2002**, *3*, 715–720.
3. Steen, K. H.; Steen, A. E.; Reeh, P. W. A Dominant Role of Acid pH in Inflammatory Excitation and Sensitization of Nociceptors in Rat Skin *In Vitro*. *J. Neurosci.* **1995**, *15*, 3982–3989.
4. Mariotto, S.; de Prati, A. C.; Cavalieri, E.; Amelio, E.; Marlinghaus, E.; Suzuki, H. Extracorporeal Shock Wave Therapy in Inflammatory Diseases: Molecular Mechanism That Triggers Anti-inflammatory Action. *Curr. Med. Chem.* **2009**, *16*, 2366–2372.
5. Turrens, J. F. Mitochondrial Formation of Reactive Oxygen Species. *J. Physiol.* **2003**, *552*, 335–344.
6. Barnham, K. J.; Masters, C. L.; Bush, A. I. Neurodegenerative Diseases and Oxidative Stress. *Nat. Rev. Drug Discovery* **2004**, *3*, 205–214.
7. Trachootham, D.; Alexandre, J.; Huang, P. Targeting Cancer Cells by ROS-Mediated Mechanisms: A Radical Therapeutic Approach? *Nat. Rev. Drug Discovery* **2009**, *8*, 579–591.
8. Jagetia, G.; Aggarwal, B. "Spicing Up" of the Immune System by Curcumin. *J. Clin. Immunol.* **2007**, *27*, 19–35.
9. Barzegar, A.; Moosavi-Movahedi, A. A. Intracellular ROS Protection Efficiency and Free Radical-Scavenging Activity of Curcumin. *PLoS One* **2011**, *6*, e26012.
10. Choi, S. W.; Zhang, Y.; Xia, Y. A Temperature-Sensitive Drug Release System Based on Phase-Change Materials. *Angew. Chem., Int. Ed.* **2010**, *49*, 7904–7908.
11. Broaders, K. E.; Grandhe, S.; Fréche, J. M. J. A Biocompatible Oxidation-Triggered Carrier Polymer with Potential in Therapeutics. *J. Am. Chem. Soc.* **2011**, *133*, 756–758.

12. Gao, N.; Zhang, Q.; Mu, Q.; Bai, Y.; Li, L.; Zhou, H.; Butch, E. R.; Powell, T. B.; Snyder, S. E.; Jiang, G.; *et al.* Steering Carbon Nanotubes to Scavenger Receptor Recognition by Nanotube Surface Chemistry Modification Partially Alleviates NFκB Activation and Reduces Its Immunotoxicity. *ACS Nano* **2011**, *5*, 4581–4591.
13. Wilson, D. S.; Dalmasso, G.; Wang, L.; Sitaraman, S. V.; Merlin, D.; Murthy, N. Orally Delivered Thioketal Nanoparticles Loaded with TNF-α-siRNA Target Inflammation and Inhibit Gene Expression in the Intestines. *Nat. Mater.* **2010**, *9*, 923–928.
14. Chiu, Y. L.; Chen, S. A.; Chen, J. H.; Chen, K. J.; Chen, H. L.; Sung, H. W. A Dual-Emission Förster Resonance Energy Transfer Nanoprobe for Sensing/Imaging pH Changes in the Biological Environment. *ACS Nano* **2010**, *4*, 7467–7474.
15. Didenko, V. V. DNA Probes Using Fluorescence Resonance Energy Transfer (FRET): Designs and Applications. *Biotechniques* **2001**, *31*, 1106–1116.
16. Ke, D.; Wang, X.; Yang, Q.; Niu, Y.; Chai, S.; Chen, Z.; An, X.; Shen, W. Spectrometric Study on the Interaction of Dodecyltrimethylammonium Bromide with Curcumin. *Langmuir* **2011**, *27*, 14112–14117.
17. Sapsford, K. E.; Granek, J.; Deschamps, J. R.; Boeneman, K.; Blanco-Canosa, J. B.; Dawson, P. E.; Susumu, K.; Stewart, M. H.; Medintz, I. L. Monitoring Botulinum Neurotoxin A Activity with Peptide-Functionalized Quantum Dot Resonance Energy Transfer Sensors. *ACS Nano* **2011**, *5*, 2687–2699.
18. Aggarwal, B. B.; Sung, B. Pharmacological Basis for the Role of Curcumin in Chronic Diseases: An Age-Old Spice with Modern Targets. *Trends Pharmacol. Sci.* **2009**, *30*, 85–94.
19. Comhair, S. A. A.; Erzurum, S. C. Antioxidant Responses to Oxidant-Mediated Lung Diseases. *Am. J. Physiol.: Lung Cell. Mol. Physiol.* **2002**, *283*, L246–L255.
20. Zhai, Z.; Gomez-Mejiba, S. E.; Gimenez, M. S.; Deterding, L. J.; Tomer, K. B.; Mason, R. P.; Ashby, M. T.; Ramirez, D. C. Free Radical-Operated Proteotoxic Stress in Macrophages Primed with Lipopolysaccharide. *Free Radicals Biol. Med.* **2012**, *53*, 172–181.
21. Lee, Y. D.; Lim, C. K.; Singh, A.; Koh, J.; Kim, J.; Kwon, I. C.; Kim, S. Dye/Peroxalate Aggregated Nanoparticles with Enhanced and Tunable Chemiluminescence for Biomedical Imaging of Hydrogen Peroxide. *ACS Nano* **2012**, *6*, 6759–6766.
22. Niikura, K.; Matsunaga, T.; Suzuki, T.; Kobayashi, S.; Yamaguchi, H.; Orba, Y.; Kawaguchi, A.; Hasegawa, H.; Kajino, K.; Ninomiya, T.; *et al.* Gold Nanoparticles as a Vaccine Platform: Influence of Size and Shape on Immunological Responses *In Vitro* and *In Vivo*. *ACS Nano* **2013**, *7*, 3926–3938.
23. Hara, M. R.; Agrawal, N.; Kim, S. F.; Cascio, M. B.; Fujimuro, M.; Ozeki, Y.; Takahashi, M.; Cheah, J. H.; Tankou, S. K.; Hester, L. D.; *et al. S*-Nitrosylated GAPDH Initiates Apoptotic Cell Death by Nuclear Translocation Following Siah1 Binding. *Nat. Cell Biol.* **2005**, *7*, 665–674.
24. Li, P.; Zhou, C.; Rayatpisheh, S.; Ye, K.; Poon, Y. F.; Hammond, P. T.; Duan, H.; Chan-Park, M. B. Cationic Peptidopolysaccharides Show Excellent Broad-Spectrum Antimicrobial Activities and High Selectivity. *Adv. Mater.* **2012**, *24*, 4130–4137.
25. Jen, M. C.; Serrano, M. C.; van Lith, R.; Ameer, G. A. Polymer-Based Nitric Oxide Therapies: Recent Insights for Biomedical Applications. *Adv. Funct. Mater.* **2012**, *22*, 239–260.
26. Wu, P.; Wang, J.; He, C.; Zhang, X.; Wang, Y.; Liu, T.; Duan, C. Luminescent Metal-Organic Frameworks for Selectively Sensing Nitric Oxide in an Aqueous Solution and in Living Cells. *Adv. Funct. Mater.* **2012**, *22*, 1698–1703.
27. Derochette, S.; Franck, T.; Mouithys-Mickalad, A.; Deby-Dupont, G.; Neven, P.; Serteyn, D. Intra- and Extracellular Antioxidant Capacities of the New Water-Soluble Form of Curcumin (NDS27) on Stimulated Neutrophils and HL-60 Cells. *Chem. Biol. Interact.* **2013**, *201*, 49–57.
28. Strimpakos, A. S.; Sharma, R. A. Curcumin: Preventive and Therapeutic Properties in Laboratory Studies and Clinical Trials. *Antioxid. Redox Signaling* **2008**, *10*, 511–545.
29. Cui, M.; Naczynski, D. J.; Zevon, M.; Griffith, C. K.; Sheihet, L.; Poventud-Fuentes, I.; Chen, S.; Roth, C. M.; Moghe, P. V. Multifunctional Albumin Nanoparticles As Combination Drug Carriers for Intra-Tumoral Chemotherapy. *Adv. Healthcare Mater.* **2013**, 10.1002/adhm.201200467.
30. Lai, Y.; Lin, L.; Pan, F.; Huang, J.; Song, R.; Huang, Y.; Lin, C.; Fuchs, H.; Chi, L. Bioinspired Patterning with Extreme Wettability Contrast on TiO_2 Nanotube Array Surface: A Versatile Platform for Biomedical Applications. *Small* **2013**, 10.1002/smll.201300187.
31. Khetani, S. R.; Bhatia, S. N. Microscale Culture of Human Liver Cells for Drug Development. *Nat. Biotechnol.* **2008**, *51*, 120–126.
32. Strasser, E. M.; Wessner, B.; Manhart, N.; Roth, E. The Relationship Between the Anti-inflammatory Effects of Curcumin and Cellular Glutathione Content in Myelomonocytic Cells. *Biochem. Pharmacol.* **2005**, *70*, 552–559.
33. Nishinaka, Y.; Aramaki, Y.; Yoshida, H.; Masuya, H.; Sugawara, T.; Ichimori, Y. A New Sensitive Chemiluminescence Probe, L-012, for Measuring the Production of Superoxide Anion by Cells. *Biochem. Biophys. Res. Commun.* **1993**, *193*, 554–559.
34. Kielland, A.; Blom, T.; Nandakumar, K. S.; Holmdahl, R.; Blomhoff, R.; Carlsen, H. *In Vivo* Imaging of Reactive Oxygen and Nitrogen Species in Inflammation Using the Luminescent Probe L-012. *Free Radicals Biol. Med.* **2009**, *47*, 760–766.
35. Chiu, Y. L.; Ho, Y. C.; Chen, Y. M.; Peng, S. F.; Ke, C. J.; Chen, K. J.; Mi, F. L.; Sung, H. W. The Characteristics, Cellular Uptake and Intracellular Trafficking of Nanoparticles Made of Hydrophobically-Modified Chitosan. *J. Controlled Release* **2010**, *146*, 152–159.
36. Sonaje, K.; Lin, K. J.; Wey, S. P.; Lin, C. K.; Yeh, T. H.; Nguyen, H. N.; Hsu, C. W.; Yen, T. C.; Juang, J. H.; Sung, H. W. Biodistribution, Pharmacodynamics and Pharmacokinetics of Insulin Analogues in A Rat Model: Oral Delivery Using pH-Responsive Nanoparticles *vs.* Subcutaneous Injection. *Biomaterials* **2010**, *31*, 6849–6858.
37. Brooks, B. R; Bruccoleri, R. E.; Olafson, B. D.; States, D. J.; Swaminathan, S.; Karplus, M. Charmm: A Program for Macromolecular Energy, Minimization, and Dynamics Calculations. *J. Comput. Chem.* **1983**, *4*, 187–217.
38. Pettersen, E. F.; Goddard, T. D.; Huang, C. C.; Couch, G. S.; Greenblatt, D. M.; Meng, E. C.; Ferrin, T. E. UCSF Chimera—A Visualization System for Exploratory Research and Analysis. *J. Comput. Chem.* **2004**, *25*, 1605–1612.
39. Kim, S.; Park, H.; Song, Y.; Hong, D.; Kim, O.; Jo, E.; Khang, G.; Lee, D. Reduction of Oxidative Stress by *p*-Hydroxybenzyl Alcohol-Containing Biodegradable Polyoxalate Nanoparticulate Antioxidant. *Biomaterials* **2011**, *32*, 3021–3029.